crystals

MDPI

Article

Collective Relaxation Processes in Nonchiral Nematics

Neelam Yadav [1], Yuri P. Panarin [1,2,*], Wanhe Jiang [3], Georg H. Mehl [3] and Jagdish K. Vij [1]

[1] Department of Electronic and Electrical Engineering, Trinity College Dublin, The University of Dublin, Dublin 2, D02 PN40 Dublin, Ireland; yadavn@tcd.ie (N.Y.); jvij@tcd.ie (J.K.V.)
[2] Department of Electrical and Electronic Engineering, Technological University Dublin, Dublin 7, D07 EWV4 Dublin, Ireland
[3] Department of Chemistry, University of Hull, Hull HU6 7RX, UK; w.jiang-2019@hull.ac.uk (W.J.); g.h.mehl@hull.ac.uk (G.H.M.)
* Correspondence: yuri.panarin@tudublin.ie

Abstract: Nematic–nematic transitions in a highly polar nematic compound are studied, in thick cells in which the molecules are aligned parallel to the substrates but perpendicular to the applied electric field, using dielectric spectroscopy in the frequency range 1 Hz to 10 MHz over a wide temperature range. The studied compound displays three nematic phases under cooling from the isotropic phase: ubiquitous nematic N; high polarizability N_X; and ferroelectric nematic N_F. Two collective processes were observed. The dielectric strength and relaxation frequency of one of the processes P_2 showed a dependence on the thickness of the cell. The process P_1 is the amplitude mode, while the process P_2 is the phason mode.

Keywords: dielectric spectroscopy; dielectric permittivity; ferroelectric nematics; chiral; relaxation processes; planar alignment; nematic–nematic transitions; liquid crystals

Citation: Yadav, N.; Panarin, Y.P.; Jiang, W.; Mehl, G.H.; Vij, J.K. Collective Relaxation Processes in Nonchiral Nematics. *Crystals* **2023**, *13*, 962. https://doi.org/10.3390/cryst13060962

Academic Editors: Stephen J. Cowling and Charles Rosenblatt

Received: 28 April 2023
Revised: 1 June 2023
Accepted: 13 June 2023
Published: 16 June 2023

1. Introduction

During the last few decades, both chirality and the polarization have been detected in liquid crystalline (LC) systems consisting of nonchiral mesogens such as the bent-core molecules under certain confinement conditions and the dimers with odd methylene spacers in between the two mesogens [1]. In these systems, achiral mesogens may lead to the so-called "chiral phases", exhibiting spontaneous polarization or the optical activity. Finally, the Ferroelectric Nematic phase was discovered in 2017, over a century after its prediction made by P. Debye [2] and M. Born [3]. Nishikawa et al. [4] reported extremely large dielectric permittivity ~10^4, and they also observed huge spontaneous polarization of ~4.4 μC cm^{-2} in the ferroelectric nematic phase of a compound DIO. DIO exhibits a variety of nematic phases on cooling from the isotropic phase termed as the conventional nematic (M1 or N), high polarizability nematic (M2 or N_X), and the ferroelectric nematic (MP or N_F) phases [5,6] in order of decreasing temperature. Initially, Mandle et al. synthesized compounds with large dipole moments: RM230, RM734 and their homologues; these exhibited two nematic mesophases, termed N and N_X, and these phases were separated by a weak first-order transition [7–10]. The polar N_X formed a splay nematic (N_S) phase [11–13]. The latter arose presumably from the wedge shape of the molecules having a splay modulation period of 5–10 microns. The N-N_S phase transition bears semblance to the ferroelectric–ferro-elastic transition that occurs via flexoelectric coupling [13]. Chen et al. demonstrated ferroelectricity for the first time in a previously labelled N_X (or N_S) phase of the nitro compound RM734, thus confirming the discovery of the ferroelectric nematic (N_F) phase that displayed intriguing electro-optical properties [14]. The compound DIO was also visited by the Boulder group in 2021 [15]. They found that the intermediate (M2 or N_X) is a density-modulated biaxial phase (existing between the paraelectric, uniaxial N, and the ferroelectric, phase, N_F), antiferroelectric and has a period of 8.8 nm. They labelled this phase the smectic Z_A (SmZ_A) antiferroelectric phase. These previously unknown

phases displayed fascinating properties, which motivated researchers internationally to understand the peculiar and interesting characteristics [16] of the new nematic phases.

It is important to understand such rarely observed novel nematic–nematic phase transitions to underpin its physics as well as harness the enormous potential of the ferroelectric nematics for applications in super capacitors as energy storage devices, non-linear optics, sensors, and photonics. The origin of the mechanism/s for the formation of the multiple nematic phases is not yet fully understood. It is worth remarking that nematic–nematic transitions have been observed so far only in a few compounds. Though a large dipole moment of a molecule is an important prerequisite, the spatial arrangement of dipoles, however, in a molecule is also an extremely important requirement. Undoubtedly, the lack of understanding of the properties of the nematic variant phases is a barrier to their use in new technologies. The library of the compounds showing the N_F phase needs to be expanded to predict the structure–property (N_F phase) characteristics.

Dielectric spectroscopy (DS) [17] is a powerful methodology for studying the dipolar response to a weak electric field without causing much disturbance to the material, and for exploring the relaxation phenomena in the liquid crystalline nematic phase under investigation. Dielectric spectroscopy has been used for investigating ferroelectric nematics: in investigating fluoro compounds with the objective of making a preliminary assignment of the processes in DIO [18]. DS has successfully been used to explore the various LC phases such as the columnar hexagonal [19,20], ferrielectric [21], ferroelectric SmC* [22], SmCP [23], and antiferroelectric SmC_A* [24], de Vries phase [25], and the bent core nematics [26].

In this paper, we investigate the dielectric properties of a compound DIO, including the study of its high-temperature paraelectric N phase. Specifically, we present a detailed analysis of the relaxation mechanisms detected in this compound in a thick cell and compare the results from a thin cell. The molecular structure and the phase transition temperatures recorded using polarizing optical microscopy at a scanning rate of 2 °C/min on cooling are given in Figure 1.

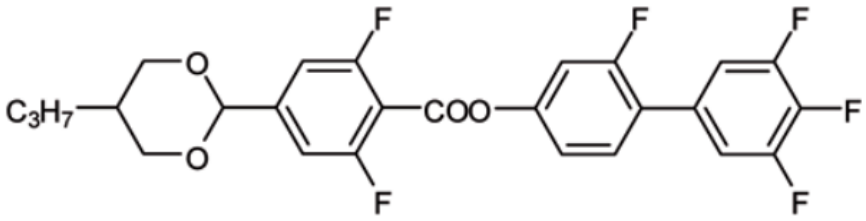

X—~35 °C—N_F—66.8 °C—N_X—83.5 °C—N—173.8 °C Iso

Figure 1. The molecular structure, the phase sequence, and the transition temperatures of the DIO compound.

2. Materials and Methods

The compound, DIO, was resynthesized at the University of Hull, Hull, UK. The real and imaginary parts of complex dielectric permittivity values are measured as a function of frequency for different temperatures using a high-resolution broadband dielectric spectrometer manufactured by Novo-control, GmbH, Germany. The LC cells for the experiments were made by gluing together of the two indium tin oxide (ITO)-coated glass substrates, separated by a spacer of thickness ~25 μm. The ITO substrates are selected to have a low sheet resistance of 10 Ω/□. The latter enables a shift in the parasitic mode to higher frequencies beyond the window of the experiment. Commercial cells procured from EHC Ltd., Japan were used for planar alignment, having a coating of the polyimide (LX-1400, Hitachi-Kasei) of ~20 nm thickness. Thick homeotropic samples were made by coating the glass plates with a polymer, AL6072. The sample was filled at a lower temperature (150 °C) in the nematic phase by capillary action and then heated quickly to its isotropic state. The dielectric permittivity measurements were made using planar and homeotropic aligned liquid crystalline sample under cooling. A low probe voltage of 0.1 V was applied across the cell and temperature was changed slowly in steps of 1 °C.

3. Results and Discussions

The variation of the permittivity and of the dielectric loss with temperature were recorded for a planarly aligned cell with a thickness of 25 μm in the frequency range of 0.1 Hz to 10 MHz. The three-dimensional spectra for permittivity and loss for a cell with planar alignment having a cell-spacing of 25 μm are shown in Figure 2. Prior to making these measurements, the samples in liquid crystal cells were placed under a polarizing optical microscope to check the quality of alignment of the mesogens in the planar configuration. Figure 3 depicts the textures captured for the planar-aligned sample in all phases. The snapshots show perfect alignment in the paraelectric nematic phases, which are the focus of the present study. In the N_X phase, numerous small domains start emerging which convert into bigger domains covering the entire area of the cell in the N_F phase. Figure 4 presents the dielectric permittivity and the dielectric loss spectra at different temperatures in the three phases: (N) 160 °C, 120 °C; (N_X) 80 °C, 70 °C; and (N_F) at 60 °C.

The recorded dielectric spectra were analyzed using WINFIT software, supplied by Novocontrol GmbH, Germany, and fitted to three relaxation processes with the objective of determining the origin of these three processes. The Havriliak–Negami Equation (1) was used to fit the experimental dielectric data on the real and the imaginary parts of the complex permittivity:

$$\varepsilon^* = \varepsilon_\infty + \sum_{j=1}^{n} \frac{\Delta\varepsilon_j}{\left[1 + (i\omega\tau_j)^{\alpha_j}\right]^{\beta_j}} - \frac{i\sigma}{\varepsilon_0\omega} \quad (1)$$

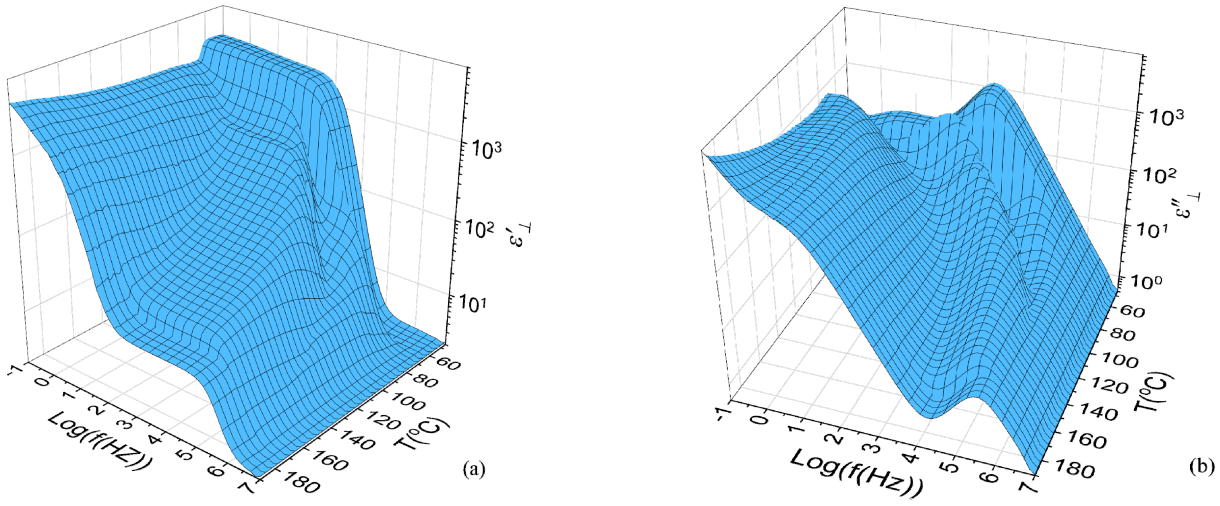

Figure 2. Three-dimensional (3D) plots of (**a**) permittivity and (**b**) dielectric loss spectra for a planar-aligned cell with a cell thickness of 25 μm.

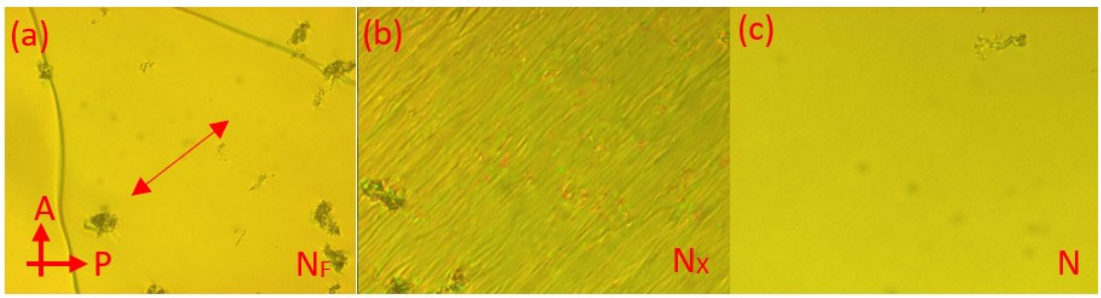

Figure 3. Textures of the DIO compound with molecules aligned planarly for a 25 μm thick cell at (**a**) 160 °C, (**b**) 80 °C, and (**c**) 60 °C, respectively. The arrow in (**a**) indicates the rubbing direction which is the same in (**b**,**c**).

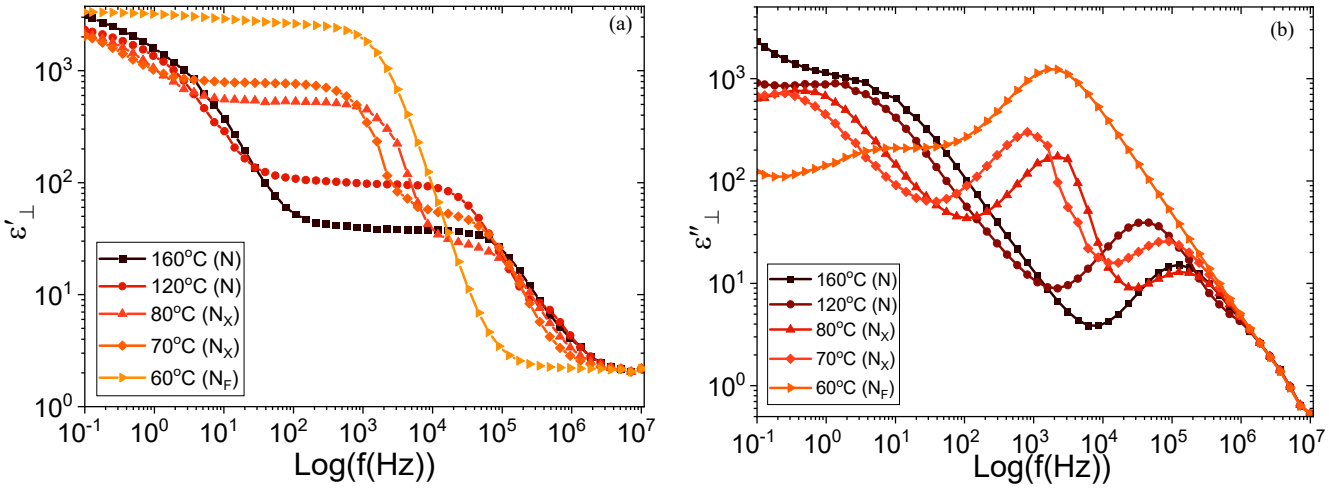

Figure 4. The variation of (**a**) dielectric permittivity and (**b**) the dielectric loss with temperature for a planar-aligned cell with a thickness of 25 μm.

The fitting of the data to Equation (1) led to the dielectric parameters of the various processes as well as the infinite frequency permittivity denoted by ε_∞. The latter permittivity is dependent on the atomic and electronic polarizabilities, ε_0 is the permittivity of free space, $\omega = 2\pi f$ is the angular frequency of the applied field, σ is the dc conductivity, τ_j is the relaxation time, $\Delta\varepsilon_j$ is the dielectric amplitude or the dielectric strength, and α_j and β_j are the symmetric and asymmetric broadening parameters determining the distribution of relaxation times of the jth relaxation process. The experimental data were fitted to the three relaxation processes; i.e., $n = 3$. The symmetrical stretching parameter of the lowest frequency relaxation process P_0 is $\alpha_0 < 1$. Hence, the mechanism is of 'the Cole–Cole type'. This process (blue curve in Figure 5a) is strongly dependent on the LC cell parameters, especially on the thickness of the alignment layer/s. We identify this process as arising from the mobility of ions since this also exists in a generic nematic LC, 5CB, where no collective relaxation processes are observed. However, the LC cells used in practice do need to incorporate alignment layers for achieving the defined orientations: planar or homeotropic. The alignment layer limits the conductivity, i.e., on the application of the external electric field, the ions in the medium (though initially distributed uniformly in the entire volume of the cell) start to migrate in the direction of the electric field, and the ionic charge continues accumulating on the surfaces of the alignment layers. On applying an AC electric field, ions in the medium respond to the alterations of the field leading to a relaxation process in the dielectric spectra. This process depends on the ionic mobility (and hence on the temperature) and the thickness of the alignment layer/s. The dielectric strength also depends on the ion's mobility, concentration, electric conductivity, thickness and the type of alignment layer/s. There are two opposite scenarios: (i) finite conductivity and (ii) zero conductivity of the material. For the first case, we can expect only a low-frequency exponential conductivity term $\left(\frac{i\sigma}{\varepsilon_0\omega}\right)$ in Equation (1). For the second case, this conductivity term should be absent, though a strong pseudo-relaxation process does arise from a separation of the ions and from the accumulation of charge on the alignment layers. This is confirmed by our experiments using a generic nematic 5CB in two cells, one without conducting layers and the second with a high resistivity SiO dielectric layer. This parasitic pseudo-process is mistakenly reported in the literature as a collective relaxation process. This in turn leads to an incorrect conclusion for the occurrence of the spontaneous polarization in an ordinary nematic phase of liquid crystals. Therefore, the lowest frequency process is mainly due to the conductivity arising from a separation of the charges and from the deposition of the ions on the polymer layers. It disappears on cooling to the N_F phase.

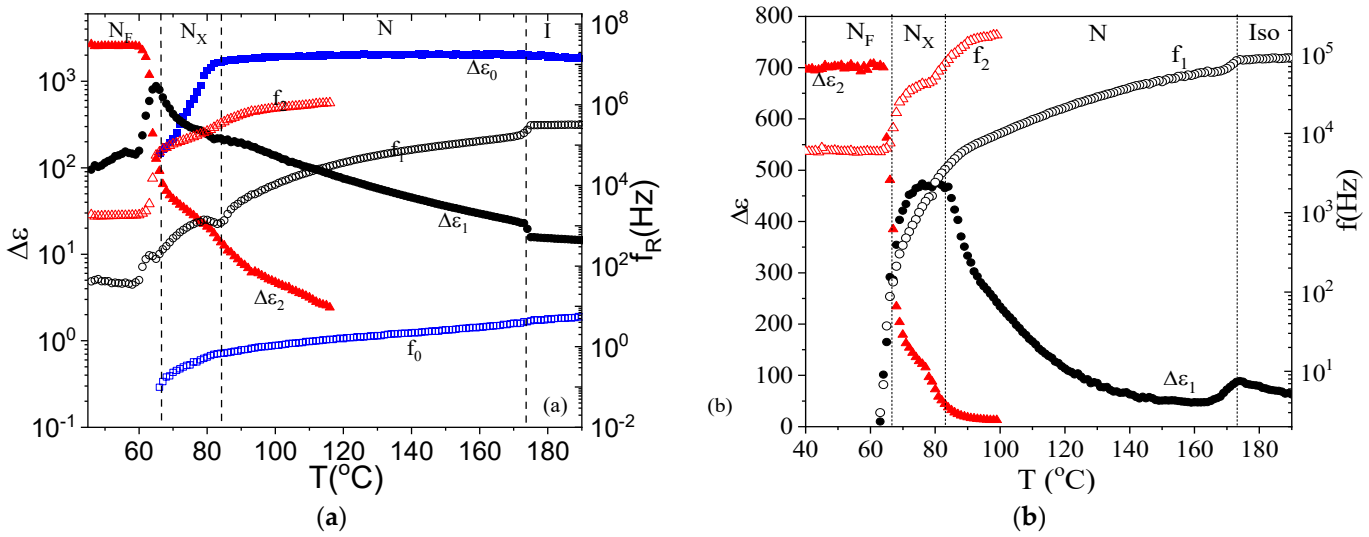

Figure 5. Planar-aligned cells. The temperature dependence of the relaxation processes: dielectric strength (Δε) (filled symbols) and the relaxation frequency (*f*) (unfilled symbols) in planarly aligned cell of (**a**) 25 μmand (**b**) 4 μmthick cell. The experimental data points are shown in color: blue (P_0), black (P_1), and red (P_2) ((**b**) [27]). Please note that especially the behavior in the thin and thick cells for process 1 are very different.

For the other two relaxation processes, P_1 and P_2, the fitting parameters are: $\alpha_j = 1$ and $\beta_j = 1$. These correspond to the Debye relaxation processes. The temperature dependencies of the relaxation processes in terms of the dielectric strength and the relaxation frequencies for the 25 μm and 4 μm thick planar-aligned cells are shown in Figure 5a,b. A comparison of Figures 2–5 shows numerous peculiar but interesting features.

- Two collective relaxation processes are observed in the high-temperature paraelectric nematic phases in contrast to those in an ordinary nematic phase. The relaxation processes are termed as P_1 and P_2 in order of the increase in the relaxation frequency and specified by the subscripts 1 and 2.
- The DC conductivity (mode P_0 in Figure 5a) in a planar-aligned cell is predominant. This gives the impression to the readers that the permittivity in the paraelectric nematic phases is also very high. However, on a careful examination and from subtracting the conductivity term from the spectra, the real value of the permittivity obtained is less in the paraelectric phases and it jumps to a higher value in the N_F phase (Figure 5a). Additionally, it is pertinent to mention here that 'dielectric parameters of the two main relaxation processes' are not affected by the conductivity.
- An extremely large value of the permittivity (~3000) was deduced from the fitting of the dielectric spectra to Equation (1) (Figure 4, parametersplotted in Figure 5a). Generally, the spectra are recorded using LC cells fabricated by sandwiching two glass substrates, having an ITO layer on each inside surface of the substrate and each surface coated by different polymers, depending on the alignment needed. The surface treatment by an aligning agent, which is polymerized on keeping the substrates in the oven for a fixed time, is a crucial step in obtaining an almost perfect alignment. Without it, one cannot be certain of the molecular alignment achieved, especially in an opaque cell, with electrodes made from a metal. In cells with the surface treatment, the total capacitance of the experimental cell depends on the relative values of the capacitance of the liquid crystalline sample (C_{LC}) and of the two alignment layers (C_P). For details on the extremely large dielectric permittivity of the confined material, see Clark et al. [28]; for $C_{LC} > C_P$, the measured capacitance is the capacitance of the two polymer layers connected in series with C_{LC}. The measured value approximates to the capacitance of the aligning layers if $C_{LC} >> C_P$, and hence, the measured value of the permittivity in the N_F phase is erroneous. Nevertheless, in the present study, as stated

above, we focus on to the collective relaxation processes in the higher temperature paraelectric phases, where the dielectric permittivity is reasonably low, and is therefore not limited by the capacitance of the alignment layers.

The variation in the dielectric strength and the relaxation frequency of the mid-frequency process P_1 with temperature is represented in Figure 5a,b (marked black). The relaxation process starts off from the isotropic phase and gradually continues increasing, under cooling, in the N_F phase in a thick cell, but it disappears in a thin cell. In the isotropic state, this mode arises from the flip-flop rotation of the mesogens around their short axes. Permittivity in the iso phase is related to $\varepsilon_{iso} = (\varepsilon_{||} + 2\varepsilon_{\perp})/3$. Hence, at the isotropic (Iso)-N phase transition temperature, the strength of the relaxation process should decrease when the molecules are planarly aligned, in agreement with the results presented in Figure 5b, for a 4 µm-thick cell This trend also agrees with the assignment as the flip-flop mode given by Sebastian et al. [13]. The dependencies of the dielectric parameters ($\Delta\varepsilon$, f) on temperature show intriguing features in the paraelectric nematic phases in thin and thick cells. In general, the dependence of the relaxation frequency on the temperature should obey the Arrhenius equation given by:

$$f(T) = A\ exp((-E_a)/RT) \quad (2)$$

According to the above equation, the log of the frequency $f(T)$ with respect to $1/T$ should be a straight line with a negative slope equal to the activation energy, E_a. The thick cell follows Arrhenius behavior in the N phase, but the sample aligned in a thin cell exhibits a different behavior, as seen for $f(T)$ for P_1, Figure 5b. Instead, a soft mode-like behavior is displayed by the temperature-dependent curve of the frequency; i.e., the relaxation frequency shows a large decrement as the $N_X$toN_F phase transition temperature is approached in a thin cell. This peculiar behavior is reminiscent of the soft mode relaxation observed at the SmA−SmC* phase transition temperature. This is attributed to an increase in the correlation length or to an increase in the tilt angle fluctuations with a decrease in temperature. On approaching the ferroelectric nematic phase, the relaxation process is due to an increase in the correlation length (hence to the correlation volume) which persists from the N_X−N_F phase transition temperature. This process can be identified as the amplitude mode. The dielectric strength in the N phase demonstrates the soft mode-like trend in a thin cell but is a straight line (as a function of $1/T$) in thick cells. The soft mode-like behavior in the N phase is found to be similar to that in the SmA phase [29]. However, in the N_F phase, the Goldstone mode dominates in the N_F phase, and it would be a challenge to find the soft mode in the N_F phase. It may be that the two modes, Goldstone and the soft in the N_F phase, cannot be easily separated. This is suggested as a problem that need to be solved in future.

The process P_2 shows almost similar behavior in both thick and thin cells. However, P_2 is not observed in the isotropic phase but it first emerges in the paraelectric nematic phase. There can be a possibility that the process P_2 is too weak in strength to be visible at higher temperatures. This explains why Brown et al. [18] observed this process only in the N_X phase, where this process is prominent and is distinguishable from the parasitic ITO peak. In our study, as mentioned before, the low sheet resistance ITO electrodes were used such that the ITO peak is moved outside the frequency range of the experiment, and the process P_2 becomes noticeable both in the thin and thick cells. The process is assigned to the phason mode.

Another interesting feature of the processes P_1 and P_2 is found from drawing a comparison of their relaxation parameters in thick and thin [27] planar cells. The dielectric parameters of P_1 are almost independent of the cell thickness, while the parameters of P_2 are dependent on the cell thickness, and hence as a thickness mode, the dielectric strength is proportional to the cell thickness, and the relaxation frequency is a reciprocal of the cell thickness, which reminds us of the so-called "thickness mode" in SSFLCs [22]. This leads

to a conclusion that that relaxation process P_1 can be an amplitude mode, while the process (P_2) is a phason mode.

Furthermore, a homeotropic cell fabricated with a cell thickness of 28 μm was also studied in a temperature range of 45–120 °C. Figure 6a represents the three-dimensional dielectric loss spectra, the corresponding dielectric parameters are plotted in Figure 6b. The dielectric relaxation strength $\Delta\varepsilon_1$ decreases in the N_X phase. The behavior of the two relaxation modes in N_X is similar to that observed by Brown et al. [18], while in thin cells [27], the process P_1 does not show any decrease in strength in the N_X phase but exhibits a sharp decrease in the N_F phase only. A comparison between thin (refer Figures 3a and 4a of [27]) and thick homeotropic cells (Figure 6a,b) shows a similar dependence on the thickness of the cell. This demonstrates that the dielectric response especially for the homeotropic aligned cell is strongly dependent on the thickness of the cell used and the conditions of molecular anchoring on the two surfaces.

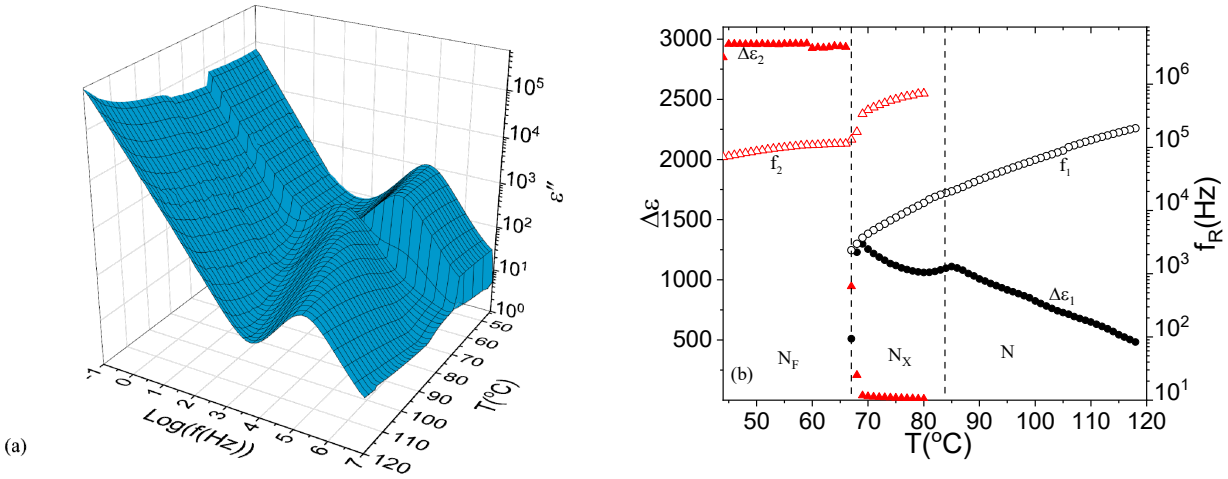

Figure 6. (**a**) Thick homeotropic cell: Three-dimensional dielectric loss spectra for a 28 μm−thick homeotropic cell and the corresponding (**b**) dielectric parameters.

4. Conclusions

In conclusion, two collective relaxation modes are observed experimentally in the paraelectric nematic phases of an achiral compound aligned both in thick planar and homeotropic cells in contrast to those seen in a conventional nematic. A decrease in $\Delta\varepsilon_1$ in the N_X phase followed by in N_F is observed in thick homeotropic cells. A sudden increase in $\Delta\varepsilon_2$ at the N_X−N_F transition signifies that the two phases, N_X and N_F, are different in nature. The dielectric parameters for the process P_2 show a variation with an increase in thickness of the cells. It is shown that the thickness of the cells and the surface anchoring conditions have profound effect on the dielectric response in nematic phases of a ferroelectric nematic compound.

Author Contributions: Y.P.P. designed the experiments. N.Y. made cells and carried out the dielectric spectroscopy measurements. Y.P.P. and N.Y. determined the dielectric parameters from the analysis of the experimental data. J.K.V., Y.P.P. and G.H.M. proposed the project. W.J. and G.H.M. synthesized the material studied. All authors contributed to writing and the editing of the manuscript. All authors have read and agreed to the published version of the manuscript.

Funding: This research was part funded by the Science Foundation Ireland, 21/US/3788 under the US-Ireland program.

Data Availability Statement: Experimental data can be obtained from the authors on request.

Acknowledgments: NY thanks the Irish Research Council for the award of the Government of Ireland PDF 2021, GOIPD/2021/858.

Conflicts of Interest: The authors declare no conflict of interest.

References

1. Panov, V.P.; Balachandran, R.; Nagaraj, M.; Vij, J.K.; Tamba, M.G.; Kohlmeier, A.; Mehl, G.H. Microsecond linear optical response in the unusual nematic phase of achiral bimesogens. *Appl. Phys. Lett.* **2011**, *99*, 261903. [CrossRef]
2. Debye, P. Einige Resultate einer kinetischen Theorie der Isolatoren. *Phys. Z.* **1912**, *13*, 97.
3. Born, M. Über anisotrope Flüssigkeiten. Versuch einer Theorie der flüssigen Kristalle und des elektrischen Kerr-Effekts in Flüssigkeiten. *Sitzungsber. Preuss. Akad Wiss.* **1916**, *30*, 614.
4. Nishikawa, H.; Shiroshita, K.; Higuchi, H.; Okumura, Y.; Haseba, Y.; Yamamoto, S.-I.; Sago, K.; Kuchi, H.K. A fluid liquid-crystal material with highly polar order. *Adv. Mater.* **2017**, *29*, 1702354. [CrossRef] [PubMed]
5. Nishikawa, H.; Araoka, F. A New Class of Chiral Nematic Phase with Helical Polar Order. *Adv. Mater.* **2021**, *2021*, 2101305. [CrossRef]
6. Li, J.; Nishikawa, H.; Kougo, J.; Zhou, J.; Dai, S.; Tang, W.; Zhao, X.; Hisai, Y.; Huang, M.; Aya, S. Development of ferroelectric nematic fluids with giant-ε dielectricity and nonlinear optical properties. *Sci. Adv.* **2021**, *7*, eabf5047. [CrossRef]
7. Mandle, R.J.; Cowling, S.J.; Goodby, J.W. Rational design of rod-like liquid crystals exhibiting two nematic phases. *Chem. A Eur. J.* **2017**, *23*, 14554. [CrossRef]
8. Mandle, R.J.; Cowling, S.J.; Goodby, J.W. A nematic to nematic transformation exhibited by a rod-like liquid crystal. *Phys. Chem. Chem. Phys.* **2017**, *19*, 11429–11435. [CrossRef]
9. Mandle, R.J.; Cowling, S.J.; Goodby, J.W. Structural variants of RM734 in the design of splay nematic materials. *Liq. Cryst.* **2012**, *48*, 1780. [CrossRef]
10. Mandle, R.J.; Sebastián, N.; Martinez-Perdiguero, J.; Mertelj, A. On the molecular origins of the ferroelectric splay nematic phase. *Nat. Commun.* **2021**, *12*, 4962. [CrossRef]
11. Takezoe, H. Polar liquid crystals—Ferro, antiferro, banana, and columnar—. *Mol. Cryst. Liq. Cryst.* **2017**, *646*, 46. [CrossRef]
12. Mertelj, A.; Cmok, L.; Sebastián, N.; Mandle, R.J.; Parker, R.R.; Whitwood, A.C.; Goodby, J.W.; Čopič, M. Splay Nematic Phase. *Phys. Rev. X* **2018**, *8*, 041025. [CrossRef]
13. Sebastián, N.; Cmok, L.; Mandle, R.J.; de la Fuente, M.R.; Olenik, I.D.; Čopič, M.; Mertelj, A. Ferroelectric-ferroelastic phase transition in a nematic liquid crystal. *Phys. Rev. Lett.* **2020**, *124*, 037801. [CrossRef]
14. Chen, X.; Korblova, E.; Dong, D.; Wei, X.; Shao, R.; Radzihovsky, L.; Glaser, M.A.; Maclennan, J.E.; Bedrov, D.; Walba, D.M.; et al. First-principles experimental demonstration of ferroelectricity in a thermotropic nematic liquid crystal: Polar domains and striking electrooptics. *Proc. Natl. Acad. Sci. USA* **2020**, *117*, 14021–14031. [CrossRef]
15. Chen, X.; Martinez, V.; Korblova, E.; Freychet, G.; Zhernenkov, M.; Glaser, M.A.; Wang, C.; Zhu, C.; Radzihovsky, L.; Maclennan, J.E.; et al. The smectic Z_A phase: Antiferroelectric smectic order as a prelude to the ferroelectric nematic. *Proc. Natl. Acad. Sci. USA* **2023**, *120*, e2217150120. [CrossRef]
16. Zhao, X.; Zhou, J.; Li, J.; Kougo, J.; Wan, Z.; Huang, M.; Aya, S. Spontaneous helielectric nematic liquid crystals: Electric analog to helimagnets. *Proc. Natl. Acad. Sci. USA* **2021**, *118*, e2111101118. [CrossRef]
17. Yadav, N.; Dhar, R. Impedance Spectroscopy. In *Modern Techniques of Spectroscopy: Basics, Instrumentation and Applications*, 1st ed.; Singh, D.K., Pradhan, M., Materny, A., Eds.; Springer: Singapore, 2021; pp. 515–540.
18. Brown, S.; Cruickshank, E.; Storey, J.M.D.; Imrie, C.T.; Pociecha, D.; Majewska, M.; Makal, A.; Gorecka, E. Multiple polar and non-polar nematic phases. *Chem. Phys. Chem.* **2021**, *22*, 2506. [CrossRef]
19. Yadav, N.; Kumar, S.; Dhar, R. Cadmium selenide quantum dots for the amelioration of the properties of a room temperature discotic liquid crystalline material. *RSC Adv.* **2015**, *5*, 78823–78832. [CrossRef]
20. Uttam, R.; Yadav, N.; Kumar, S.; Dhar, R. Strengthening of columnar hexagonal phase of a room temperature discotic liquid crystalline material by using ferroelectric barium titanate nanoparticles. *J. Mol. Liq.* **2019**, *294*, 111609. [CrossRef]
21. Panarin, Y.P.; Xu, H.; Mac Lughadha, S.T.; Vij, J.K.; Seed, A.J.; Hird, M.; Goodby, J.W. An investigation of the field-induced ferrielectric subphases in antiferroelectric liquid crystals. *J. Phys. Condens. Mater.* **1995**, *7*, L351. [CrossRef]
22. Panarin, Y.P.; Kalmykov, Y.P.; Mac Lughadha, S.T.; Xu, H.; Vij, J.K. Dielectric Dielectric response of surface stabilized ferroelectric liquid crystal cells. *Phys. Rev. E* **1994**, *50*, 4763. [CrossRef] [PubMed]
23. Sreenilayam, S.P.; Panarin, Y.P.; Vij, J.K.; Lehmann, A.; Poppe, M.; Tschierske, C. Development of ferroelectricity in the smectic phases of 4-cyanoresorcinol derived achiral bent-core liquid crystals with long terminal alkyl chains. *Phys. Rev. Mater.* **2017**, *1*, 035604. [CrossRef]
24. Panarin, Y.P.; Kalinovskaya, O.E.; Vij, J.K. The investigation of the relaxation processes in antiferroelectric liquid crystals by broad band dielectric and electro-optic spectroscopy. *Liq. Cryst.* **1998**, *25*, 241. [CrossRef]
25. Yadav, N.; Panov, V.P.; Swaminathan, V.; Sreenilayam, S.P.; Vij, J.K.; Perova, T.S.; Dhar, R.; Panov, A.; Rodriguez-Lojo, D.; Stevenson, P.J. Chiral smectic-A and smectic-C phases with de Vries characteristics. *Phys. Rev. E* **2017**, *95*, 062704. [CrossRef]
26. Sreenilayam, S.P.; Panarin, Y.P.; Vij, J.K. Dielectric study of liquid crystals with large electroclinic effect. *Mol. Cryst. Liq. Cryst.* **2015**, *610*, 63. [CrossRef]

27. Yadav, N.; Panarin, Y.P.; Vij, J.K.; Jiang, W.; Mehl, G.H. Two mechanisms for the formation of the ferronematic phase studied by dielectric spectroscopy. *J. Mol. Liq.* **2023**, *378*, 121570. [CrossRef]
28. Clark, N.A.; Chen, X.; Maclennan, J.E.; Glaser, M.A. Dielectric spectroscopy of ferroelectric nematic liquid crystals: Measuring the capacitance of insulating interfacial layers. *arXiv* **2022**, arXiv:2208.09784.
29. Kocot, A.; Wrzalik, R.; Vij, J.K.; Brehmer, M.; Zentel, R. Dielectric and electro-optical studies of a ferroelectric copolysiloxane. *Phys. Rev. B* **1994**, *50*, 16346. [CrossRef]